Geophysical Research Letters

RESEARCH LETTER
10.1029/2023GL104002

Decoupled Zircon Si–O Isotopes Tracing the Supracrustal Silicification and Komatiitic-Derived Fluids in the Source of TTGs

Kai Lei[1,2], Hao Wang[1,2], Xiaolei Wang[3], Qing Zhang[1], and Xian-Hua Li[1,2]

[1]State Key Laboratory of Lithospheric Evolution, Institute of Geology and Geophysics, Chinese Academy of Sciences, Beijing, China, [2]College of Earth and Planetary Sciences, University of Chinese Academy of Sciences, Beijing, China, [3]State Key Laboratory for Mineral Deposits Research, School of Earth Sciences and Engineering, Nanjing University, Nanjing, China

Key Points:

- Elevated $\delta^{30}Si$ and $\delta^{18}O$ values of Archean granitic continental rocks indicate the involvement of a supracrustal silicified source
- Mantle-like $\delta^{18}O$ values of Archean granitic continental rocks may have been caused by low-$\delta^{18}O$ fluid released from komatiitic rocks
- Mantle-like $\delta^{18}O$ values of Archean granitoids might not reflect the absence of supracrustal materials

Supporting Information:

Supporting Information may be found in the online version of this article.

Correspondence to:

X.-H. Li,
lixh@gig.ac.cn

Citation:

Lei, K., Wang, H., Wang, X., Zhang, Q., & Li, X.-H. (2023). Decoupled zircon Si–O isotopes tracing the supracrustal silicification and komatiitic-derived fluids in the source of TTGs. *Geophysical Research Letters*, *50*, e2023GL104002. https://doi.org/10.1029/2023GL104002

Received 4 APR 2023
Accepted 2 AUG 2023

Abstract The tonalite–trondhjemite–granodiorite suites (TTGs) are key components of the Archean continental crust and therefore crucial to the understanding of the evolution of the early Earth. Here, we present in situ zircon Si–O isotope data of TTGs from Barberton. Results show that the 3.45–3.42 Ga (Group 1) and 3.24–3.23 Ga TTGs (Group 2) have elevated $\delta^{30}Si_{melt}$ values but mantle-like $\delta^{18}O_{zrc}$ values, whereas the 3.23–3.22 Ga TTGs (Group 3) have coupled elevated $\delta^{30}Si_{melt}$ and $\delta^{18}O_{zrc}$ values relative to mantle-derived rocks. We suggest that the Group 1 and 2 TTGs had a silicified source that was affected by low-$\delta^{18}O$ fluid released from the komatiitic rocks. The low-$\delta^{18}O$ fluid decreased the $\delta^{18}O_{zrc}$ values of Group 1 and 2 TTGs but had negligible influence on their $\delta^{30}Si_{melt}$ values. The Group 3 TTGs were generated solely from the silicified source, as the low-$\delta^{18}O$ fluid had become exhausted at that time.

Plain Language Summary The Archean granitic continents are dominated by tonalite–trondhjemite–granodiorite suites (TTGs) that are generated from the partial melting of hydrous basaltic rocks. The genesis of TTGs is controversial, as the source of water is unclear. Si and O isotopes are effective indicators of the water source and should be covariant. However, in this study, we discovered both decoupled enriched Si but mantle-like O isotopic compositions, and coupled enriched Si–O isotopic compositions of TTGs from the Barberton region. We suggest that the decoupled Si–O isotope compositions resulted from the involvement of both supracrustal silicified materials and fluid released from komatiitic rocks, and that the coupled Si–O isotopic compositions were produced by the silicified materials only. The results indicate that TTGs have more variable sources than previously thought.

1. Introduction

Archean Earth has unique crustal rock associations composed of supracrustal greenstone rocks and sodic granite domes dominated by tonalite, trondhjemite, and granodiorite suites (TTGs) (Moyen & Martin, 2012). Given their dominant occurrence in present Archean continental crust, TTGs have been widely investigated to understand the geodynamic process of early Earth. In addition, as the products of crystallization from Si-saturated magma, TTGs contain abundant zircon, which is highly resistant to secondary alteration and preserves a reliable record of isotope compositions and U–Pb isotope chronology (e.g., Valley et al., 2005). Although there is a general consensus that TTGs were formed by the partial melting of hydrous basaltic protoliths (e.g., Johnson et al., 2017; Moyen & Martin, 2012), the water source and genesis of TTGs remain uncertain.

Oxygen (O) isotope is a sensitive tracer of water sources (e.g., Eiler, 2001; Trail et al., 2018; Valley et al., 2005), as the positive and negative shrifts of $\delta^{18}O$ values in TTGs relative to mantle values indicate the contribution of supracrustal materials that underwent surface water-rock interactions at variable temperatures (e.g., Johnson et al., 2022; Reimink et al., 2014; Smithies et al., 2021; Valley et al., 2005; Wang, Yang, et al., 2022; Wang, Tang, et al., 2022). Archean TTGs are characterized by enrichment in heavy Si isotopes (André et al., 2019, 2022; Deng et al., 2019; Guitreau et al., 2022; Zhang et al., 2023), possibly inherited from the precipitation of Archean Si-saturated seawater (André et al., 2019, 2022; Deng et al., 2019; Trail et al., 2018). A paradox is that although silicification is theoretically accompanied by the fractionation of O isotopes, not all Archean TTGs display O isotope compositions that differ from the mantle composition (e.g., Smithies et al., 2021; Wang, Tang,

et al., 2022). Therefore, it is necessary to integrate the Si and O isotopic systematics of TTGs to explore whether they are coupled or not.

In this study, we conducted in situ zircon Si and O isotope analyses of ca. 3.4–3.2 Ga TTGs from the Barberton granitoid–greenstone terrane in the Kaapvaal Craton. Our work reveals a shift from decoupled to coupled Si–O isotopic systematics for these TTGs, indicating varied sources comprising a silicified source and fluid released from komatiitic rocks.

2. Geologic Setting and Samples

The Kaapvaal Craton located in southeastern Africa is one of the best-preserved Archean crustal segments worldwide and has a geological record extending back to ca. 3.6 Ga (Kröner & Hofmann, 2019). The Barberton granitoid–greenstone terrane in northeastern Kaapvaal Craton is a typical ancient continental nucleus (Figure S1 in Supporting Information S1). The granitoid rocks in this terrane consist mainly of TTG domes dominated by rock associations of sodic trondhjemite and tonalite, with three stages of TTG formation at ca. 3.5, 3.4, and 3.2 Ga (Moyen et al., 2007). Since ca. 3.1 Ga, the granitoid rocks have been transformed into potassic granites (Moyen et al., 2007). The greenstone belts surrounding the granitoid domes include volcanic, sedimentary, and some intrusive rocks with ages ranging from ca. 3.5 to ca. 3.2 Ga and are traditionally divided into three main lithostratigraphic units: the Onverwacht, Fig Tree, and Moodies groups (from base to top; Figure S1 in Supporting Information S1; Lowe & Byerly, 2007; Kröner & Hofmann, 2019). In this study, 10 representative TTG samples previously dated into age groups of 3.46–3.42, 3.26–3.23, and 3.23–3.22 Ga (Wang et al., 2019, 2020; Wang, Tang, et al., 2022) were selected for geochemical and isotopic analyses (Figure S1 in Supporting Information S1). These samples consist predominantly of various proportions of plagioclase, quartz, biotite, and minor K-feldspar with accessory minerals including Fe–Ti oxides, titanite, zircon, epidote, and chlorite (Wang et al., 2020). Zircon U–Pb ages, and some of the major- and trace-element compositions and zircon O isotopes presented here have been reported previously by Wang et al. (2019, 2020) and Wang, Tang, et al. (2022).

3. Methods

Major- and trace-element contents of two samples (14SA14 and 16SA13) were measured using an AXIOS Minerals X-ray fluorescence spectrometer and an Agilent 7500a quadrupole inductively coupled plasma–mass spectrometer, respectively, at the Institute of Geology and Geophysics, Chinese Academy of Sciences (IGG-CAS) in Beijing. In order to identify the most concordant (<5% discordant) zircon grains from the samples 14SA14, 15SA10, and 16SA13 that were previously dated by Wang et al. (2019, 2020), SIMS zircon U–Pb dating was conducted again for these three samples in this study using a CAMECA IMS-1280HR SIMS (Secondary Ion Mass Spectrometry) at the IGG-CAS in Beijing, following a similar procedure described by Li et al. (2009). Zircon Si isotopes were measured using a CAMECA IMS-1280 SIMS at the IGG-CAS in Beijing, following the methods described by Liu et al. (2019). Zircon O isotopes were measured using a CAMECA IMS-1280 SIMS also at the IGG-CAS, and a CAMECA IMS-1280HR SIMS at the Beijing Research Institute of Uranium Geology, following the methods described by Li et al. (2010). Detailed descriptions of the methods can be found in Supporting Information S1 (Guitreau et al., 2020; Li et al., 2009, 2010, 2013; Liu et al., 2019, 2022; Vermeesch, 2018; Wiedenbeck et al., 2004).

4. Results

The analytical data of this study and further supporting information are provided in Figures S2–S3 in Supporting Information S1 and Tables S1–S5 in Supporting Information S1 (Lei et al., 2023).

The TTG samples can be divided into three groups on the basis of Si–O isotope characteristics and crystallization ages (Figure 1). Most zircon grains from the Group 1 TTGs (3.44–3.42 Ga) have $\delta^{18}O_{zrc}$ values ranging from 4.53‰ ± 0.25‰ (2SE) to 5.97‰ ± 0.18‰ (2SE) which are broadly similar to the mantle-derived $\delta^{18}O_{zrc}$ values (5.3‰ ± 0.6‰, 2SD, Valley, 2003), except for one grain with a $\delta^{18}O_{zrc}$ value of 6.25‰ ± 0.22‰ (2SE) (Figure 1a). These zircons have $\delta^{30}Si_{zrc}$ values between −0.41‰ ± 0.10‰ (2SE) and −0.10‰ ± 0.10‰ (2SE) (Figure 1b). The Group 2 TTGs (3.24–3.23 Ga) also have mantle-derived $\delta^{18}O_{zrc}$ values ranging from 4.51‰ ± 0.20‰ (2SE) to 5.82‰ ± 0.22‰ (2SE), except for two grains with $\delta^{18}O_{zrc}$ values of 6.14‰ ± 0.15‰ (2SE) and 3.94 ± 0.18‰ (2SE) (Figure 1a). Their $\delta^{30}Si_{zrc}$ values range from −0.46‰ ± 0.11‰ (2SE) to −0.18‰ ± 0.10‰ (2SE) (Figure 1b). The Group 3 TTGs (3.23–3.22 Ga) have $\delta^{18}O_{zrc}$ values ranging from 5.77‰ ± 0.18‰ (2SE) to 7.07‰ ± 0.12‰ (2SE), which are overall higher than the mantle-derived values to

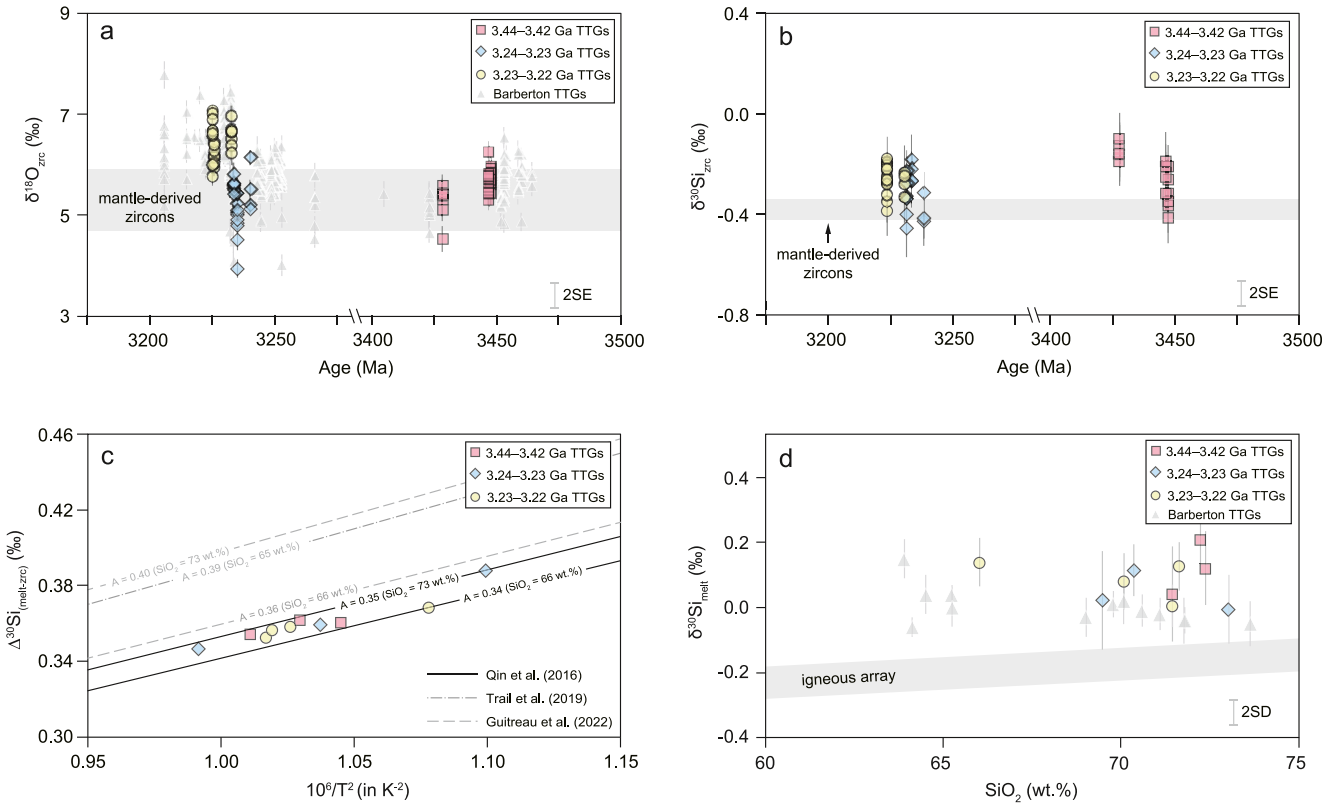

Figure 1. Si and O isotope compositions of the studied Barberton TTGs. (a and b) Zircon $\delta^{18}O$ and $\delta^{30}Si$ values versus zircon Pb–Pb ages. The gray field in each diagram represents the range of mantle zircon values ($\delta^{18}O_{zrc} = 5.3‰ \pm 0.6‰$; Valley, 2003; $\delta^{30}Si = -0.38‰ \pm 0.04‰$; Trail et al., 2018). Some $\delta^{18}O$ data of the studied TTGs and other Barberton TTGs (gray triangles) are from Wang, Tang, et al. (2022). (c) Comparison of fractionation factors calibrated by first-principles calculations (Qin et al., 2016), experiments (Trail et al., 2019), and natural observations (Guitreau et al., 2022). $\Delta^{30}Si_{(melt-zrc)}$ values were calculated by first principles with the minimum A (slop factor) values. (d) The $\delta^{30}Si_{melt}$ values of TTGs plot against their SiO_2 contents. The presented $\delta^{30}Si_{melt}$ values were calculated by first principles (Qin et al., 2016). The gray field represents the "igneous array" of Savage et al. (2011) with two standard errors. Gray triangles represent data for 3.51–3.23 Ga Barberton TTGs from André et al. (2019).

varying degrees (Figure 1a). Their $\delta^{30}Si_{zrc}$ values range from $-0.39‰ \pm 0.10‰$ to $-0.18‰ \pm 0.07‰$ (Figure 1b), similar to those of the groups 1 and 2 TTGs.

5. Discussion

5.1. Silicified Source of Barberton TTGs

Both the 3.45–3.42 Ga and 3.24–3.23 Ga TTGs have $\delta^{18}O_{zrc}$ values mostly in the range of mantle-derived zircon, whereas the 3.23–3.22 Ga TTGs have elevated zircon $\delta^{18}O_{zrc}$ values (Figure 1a). Such a positive shift of $\delta^{18}O_{zrc}$ values might indicate the involvement of supracrustal materials that underwent low-temperature water–rock interaction in the sources of the TTGs since ca. 3.2 Ga (Wang, Tang, et al., 2022). It is noted, however, that the $\delta^{30}Si_{zrc}$ values of the studied Barberton TTGs show no apparent shift at this age (Figure 1b). The Barberton TTGs have consistently high $\delta^{30}Si_{zrc}$ values relative to mantle-derived zircons (Figure 1b), but it is uncertain whether their sources contained silicified materials, as the Si isotope fractionation between zircon and melt ($\alpha_{melt-zrc}$) differs between different granite types (Guitreau et al., 2022; Trail et al., 2019). Therefore, it is necessary to calculate the melt $\delta^{30}Si$ values of the TTGs, which can be compared with the "igneous array" defined by an evolved trend of whole-rock $\delta^{30}Si$ values of most Phanerozoic mantle-derived igneous rocks with different SiO_2 contents (Savage et al., 2011).

Values of $\alpha_{melt-zrc}$ are sensitive to crystallization temperature and melt silica content, and are typically described as follows:

$$1000 \ln \alpha_{melt-zrc} = \frac{A \times 10^6}{T^2} \quad (1)$$

where A is a constant that is positive correlated with the SiO_2 contents of melt, and T is temperature in K. Values of A were calibrated from various methods, including first-principles calculations (Qin et al., 2016), experiments (Trail et al., 2019), and natural observations (Guitreau et al., 2022). Values of A and corresponding $\Delta^{30}Si_{(melt-zrc)}$ calculated by different methods are compared in Figure 1c, which shows that the lower limit of A values is constrained by first-principles calculations for our samples (Qin et al., 2016), with A values ranging from 0.34 to 0.35 at SiO_2 = 66 and 73 wt.%, respectively (Figure 1c; Table S5 in Supporting Information S1). The corresponding $\Delta^{30}Si_{(melt-zrc)}$ and $\delta^{30}Si_{melt}$ values are calculated using the mean $\delta^{30}Si_{zrc}$ values and zircon saturation temperatures (Boehnke et al., 2013), which range from 0.35 to 0.39‰ (Figure 1c), and 0.00–0.21‰ (Figure 1d), respectively. Such $\Delta^{30}Si_{(melt-zrc)}$ and $\delta^{30}Si_{melt}$ values are slightly lower than those of natural observations by ~0.03–0.05 ‰ (e.g., Guitreau et al., 2022; Trail et al., 2018; Table S5 in Supporting Information S1). Importantly, even the minimum estimation of $\delta^{30}Si_{melt}$ values calculated from first principles is higher than $\delta^{30}Si$ values of "igneous array" rocks (Figure 1d), indicating the enrichment of heavy Si isotopes in Barberton TTGs.

The heavy Si isotope compositions of Barberton TTGs may be a result of the fractional crystallization or the involvement of silicified materials in the source. The crystallization temperature of zircons depends on the aluminum saturation index (ASI) (Boehnke et al., 2013; Watson & Harrison, 1983). In short, the decrease in ASI will cause zircon to crystallize at lower temperatures and further result in high $\delta^{30}Si_{melt}$ values. However, there is no correlation between values of A/CNK [molar $Al_2O_3/(Na_2O + CaO + K_2O)$] and SiO_2 values of Barberton TTGs (Figure S4a in Supporting Information S1), indicating that there is no significant fractionation of minerals with various ASI values. In contrast to most Phanerozoic igneous rocks, Archean TTG could have been derived from the differentiation of hydrous basaltic magma under water-saturated conditions (e.g., Kleinhanns et al., 2003; Liou & Guo, 2019; Müntener et al., 2001), in which garnet incorporated with light Si isotopes (Méheut & Schauble, 2014; Yu et al., 2018) became part of the cumulate residue. In this scenario, $\delta^{30}Si_{melt}$ values would increase, accompanied by the strong fractionation of light rare earth elements (e.g., La) relative to heavy rare earth elements (e.g., Yb). However, no correlation of La_N/Yb_N ratios and $\delta^{30}Si_{melt}$ values is observed for the Barberton TTGs (Figure S4b in Supporting Information S1), demonstrating that the elevated $\delta^{30}Si_{melt}$ values did not result from the fractional crystallization of hydrous basaltic magma (e.g., André et al., 2019). The occurrence of magmatic differentiation (e.g., the fractional crystallization of biotite), as revealed by Harker diagrams that show good correlations for some major elements (particularly TiO_2, Al_2O_3, Fe_2O_3, MgO, and P_2O_5) with SiO_2 contents (Figure S5 in Supporting Information S1), would cause the evolved melts with SiO_2 contents from 66 to 73 wt.% to exhibit higher $\delta^{30}Si_{melt}$ values by ~0.05‰ (Savage et al., 2011). However, such limited change generally is negligible compared to other factors and is not easy to be detected. Therefore, the Barberton TTGs have similar $\delta^{30}Si_{melt}$ values regardless of their SiO_2 contents (Figure 1d). Integrating the above evidence, we propose that the elevated $\delta^{30}Si_{melt}$ values of the Barberton TTGs were not produced by fractional crystallization but instead reflect their silicified source.

5.2. Coupled Si–O Isotope Systematics of the Barberton TTGs

The covariation of Si and O isotopes during fluid alteration and precipitation processes have been investigated previously (e.g., Chowdhury et al., 2023; Deng et al., 2019; Trail et al., 2018; Yu et al., 2018, 2023), which have proposed three evolution paths of the coupled Si–O isotopic variations. First, pelitic sediments have relatively low $\delta^{30}Si$ but high $\delta^{18}O$ values, indicating desilicification by chemical weathering (Trail et al., 2018). Second, the $\delta^{30}Si$ values of altered rocks that underwent hydration without silicification (e.g., serpentinization) are dominated by igneous minerals, whereas $\delta^{18}O$ values vary with the alteration temperature (Abraham et al., 2011; Savage et al., 2013; Yu et al., 2018, 2023). Third, the seawater-derived authigenic silicification (e.g., chert) and seafloor silicification (e.g., silicified basalt) at low temperatures result in the enrichment of both heavy Si and heavy O isotopes (Abraham et al., 2011; Trail et al., 2018). Archean seawater was Si-saturated on account of high-temperature hydrothermal Si inputs (André et al., 2022; Robert & Chaussidon, 2006) and a lack of large-scale biosilification outputs (André et al., 2019, 2022; Deng et al., 2019). Moreover, Archean seawater was enriched in ^{30}Si, as demonstrated by the high $\delta^{30}Si$ values of silicified seafloor since ca. 3.8 Ga (André et al., 2006; Figures 2a and 2b). Therefore, we propose that the coupled elevated $\delta^{30}Si$ and $\delta^{18}O$ values of Group 3 (3.23–3.22 Ga) TTGs resulted from the partial melting of seafloor basalts with the addition of silicified materials (e.g., André et al., 2019; Deng et al., 2019).

5.3. Decoupled Si–O Isotope Systematics of the Barberton TTGs

The decoupled Si–O isotope systematics (i.e., the elevated $\delta^{30}Si$ values but mantle-like $\delta^{18}O_{zrc}$ values) of Group 1 (3.45–3.42 Ga) and Group 2 (3.24–3.23 Ga) TTGs have not been documented in previous studies. Silicified

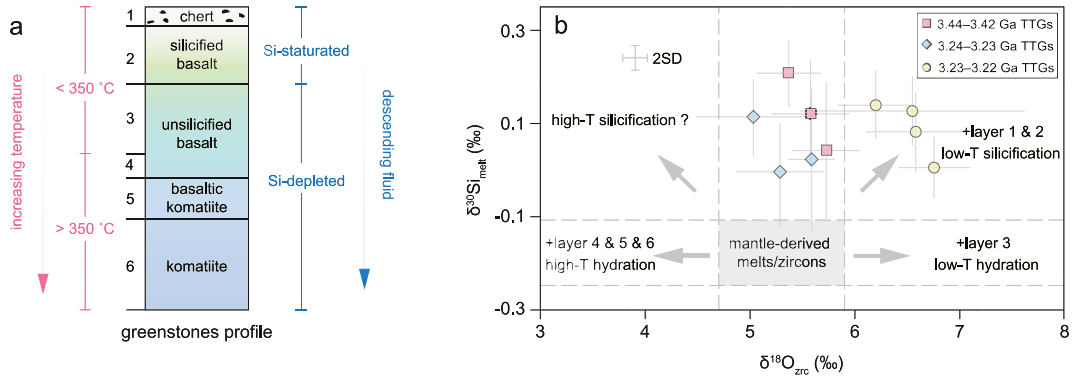

Figure 2. Covariant $\delta^{30}Si_{melt}$ and $\delta^{18}O_{zrc}$ values of TTGs and greenstone rocks. (a) Simplified typical profile of greenstones (modified from Abraham et al., 2011; André et al., 2022; Lowe & Byerly, 2007). (b) Covariant diagram of $\delta^{30}Si_{melt}$ and $\delta^{18}O_{zrc}$ (modified from Trail et al., 2018). Mean $\delta^{18}O_{zrc}$ and calculated $\delta^{30}Si_{melt}$ values for each sample are presented. The $\delta^{30}Si_{melt}$ values of mantle-derived melts were calculated as follows: $\delta^{30}Si$ (‰) = 0.0056 × SiO_2 (wt. %) − 0.567, with an uncertainty of ±0.05‰ (Savage et al., 2011). SiO_2 contents were set from 66 to 73 wt.% to encompass the compositions of studied TTGs.

seafloor that has been altered at low-temperature should have heavy O isotopic compositions ($\delta^{18}O$ > 10 ‰, Abraham et al., 2011). Thus, to generate the mantle-like $\delta^{18}O_{zrc}$ values measured for the 3.45–3.42 Ga and 3.24–3.23 Ga TTGs, an additional end-member with low $\delta^{18}O$ values is required. Low-$\delta^{18}O$ magmatic rocks are commonly associated with rifts, oceanic ridges, plume-related volcanisms, and impact craters (e.g., Johnson et al., 2022; Pope et al., 2013; Troch et al., 2020), in which meteoric water or seawater interacts with rocks at temperatures of >350°C (e.g., Valley, 2003). Low-$\delta^{18}O$ materials can contribute to the formation of TTGs in various ways, including the assimilation of low-$\delta^{18}O$ materials at shallow crustal levels, such as at Iceland or Yellowstone (e.g., Hammerli et al., 2018; Reimink et al., 2014), and the addition of low-$\delta^{18}O$ materials in melting sources (e.g., Vho et al., 2020). However, the former process during magma emplacement is less likely to have occurred in the present case because the zircons of this study show single-stage magmatic growth (Figure S2 in Supporting Information S1) and commonly have a limited $\delta^{18}O_{zrc}$ range for each sample (Figure 1a). Therefore, the relatively low-$\delta^{18}O$ signatures of some TTGs are likely to have been inherited from their sources.

Rocks in greenstone belts are generally considered the melting source of TTGs (e.g., Smithies et al., 2021). The Barberton greenstone belts can be roughly divided into several layers from top to bottom: chert, silicified basalt, unsilicified basalt, basaltic komatiite, and komatiite (Figure 2a; e.g., Abraham et al., 2011; Lowe & Byerly, 2007). As discussed above, the chert and silicified basalt have coupled heavy Si and O isotope compositions, and are likely to have been involved in the generating of Group 3 TTGs (Figure 2b). The upper part of unsilicified basalts has elevated $\delta^{18}O$ but mantle-like $\delta^{30}Si$ values (Abraham et al., 2011). This Si–O isotope composition is crucial, as it indicates that the descending fluid in this layer was depleted in Si (Abraham et al., 2011). Light Si isotopes are preferentially incorporated into precipitated minerals in water bodies (Frings et al., 2016; van den Boorn et al., 2007, 2010). Although the downward increase in temperature would have led to a decrease in the Si isotope fractionation factor between water and silica (Méheut et al., 2007, 2009), residual solutions and successive precipitates would still have had relatively high $\delta^{30}Si$ values during progressive precipitation (Abraham et al., 2011). This expectation contradicts the mantle-like $\delta^{30}Si$ values of unsilicified basalts, illustrating that precipitation had terminated despite the high $\delta^{30}Si$ values of fluids. In contrast, the O isotopes of the deep layer were still undergoing temperature-dependent fractionation, as the fluid had high hydroxyl contents and thus high O/Si ratios. A similar process to that inferred for the profile of Barberton greenstone belts occurs in the modern oceanic crust. Although modern seawater has higher $\delta^{30}Si$ values than fresh MORB (middle ocean ridge basalt) and bulk silicate Earth, most oceanic basalts and serpentinized rocks have Si isotope compositions similar to the mantle value regardless of their high or low $\delta^{18}O$ values (Savage et al., 2011; Yu et al., 2018), with the exception being the lighter Si isotopes of small portions of oceanic crust that have undergone strong low-temperature alteration (e.g., Yu et al., 2023). Si isotopes are resistant to water–rock interaction because modern seawater is deficient in Si and thus cannot cause resolvable Si isotopic variation at the bulk-rock scale. In view of the fluid being depleted in Si in the unsilicified layer, the basaltic komatiite and komatiite in deep layers where the alteration temperature exceeds 350°C are predicted to have mantle-like $\delta^{30}Si$ but low-$\delta^{18}O$ values (Figures 2a and 2b) and are inferred to

be a potential source of the low-$\delta^{18}O$ fluids that generated the 3.45–3.42 Ga and 3.24–3.23 Ga TTGs. In fact, this prediction has been demonstrated with reference to the Barberton komatiites, which display $\delta^{30}Si$ and $\delta^{18}O$ values of −0.31‰ to −0.24‰ (Deng et al., 2019) and 3.3–3.7‰ (Byerly et al., 2017; Wang et al., 2023), respectively.

As well as the low-$\delta^{18}O$ Barberton komatiites, low-$\delta^{18}O$ values in Archean zircons have been reported for cordierite–orthopyroxene granulites in the Yilgarn Craton (Hammerli et al., 2018), the tonalitic gneiss rock unit within the Acasta Gneiss Complex (Reimink et al., 2014), and amphibolites and metatonalite from Pilbara Craton (Johnson et al., 2022). Although there are different opinions on the factors that give rise to a high geothermal gradient, the high-temperature hydrothermal alteration recorded by these zircons is considered to occur in shallow levels. Except for a few special cases (e.g., giant impacts; Johnson et al., 2022), these supracrustal low-$\delta^{18}O$ rocks cannot readily contribute to the formation of TTGs because of preservation bias (Hammerli et al., 2018). Low-$\delta^{18}O$ rocks at shallow levels are readily destroyed (Hammerli et al., 2018), and their low-$\delta^{18}O$ signatures are likely overprinted by the low-temperature interaction between seawater and rocks, so long as they have not risen above sea level and subaerially exposed. Moreover, although a high-temperature alteration in Archean Si-saturated seawater can result in low $\delta^{18}O$ values, the $\delta^{30}Si$ values of these natural samples are still unknown. Therefore, basaltic komatiite and komatiite in Barberton are the likely low-$\delta^{18}O$ source for the TTGs.

Basaltic komatiite and komatiite have a strong ability to preserve water (Hartnady et al., 2022; Tamblyn et al., 2023). Most komatiitic rocks are erupted underwater and thus undergo interaction with seawater, as evidenced by the pillow structures of komatiitic rocks (e.g., Arndt et al., 2008). Although the low-$\delta^{18}O$ values of olivine in the Barberton komatiite were suggested to represent the early Earth mantle heterogeneity (Byerly et al., 2017), these low $\delta^{18}O$ values are likely from secondary minerals (e.g., serpentine) that are inevitably incorporated in olivine grains (Wang et al., 2023). Therefore, the low-$\delta^{18}O$ values of komatiitic rocks also reveal a hydration event. Crucially, thermodynamic simulations have indicated that the high MgO content of basaltic komatiite and komatiite can stabilize hydrous minerals such as chlorite and tremolite until the temperature reaches 680–800°C (Hartnady et al., 2022; Tamblyn et al., 2023). Up to 5 wt.% fluid can be extracted during dehydration at such high temperatures, which may promote the melting of overlying basaltic rocks (Hartnady et al., 2022; Tamblyn et al., 2023). $\delta^{18}O$ fractionation modeling shows that the $\delta^{18}O$ values of overlying basalt affected by the komatiitic-derived fluid can decrease 0.6–1.1‰, assuming a fluid/rock ratio of 0.1, and a fluid $\delta^{18}O$ value of 4.5 ‰ (Vho et al., 2020). This means the low-$\delta^{18}O$ fluid extracted from the basaltic komatiite and komatiite is a significant material in the melting source for the TTGs with decoupled Si–O isotope compositions. The Si isotope composition of overlying basaltic rocks might not be substantially affected by fluid derived from komatiitic rocks, as Si isotopes were resistant to metamorphic and metasomatic processes (André et al., 2006; Yu et al., 2018, 2023). Moreover, the Si isotope fractionation factor between rock and fluid is very low at temperatures of 680–800°C, and basaltic komatiite and komatiite have similar $\delta^{30}Si$ values (−0.31‰ to −0.24‰) to those of basalt (ca. −0.27 ‰; Savage et al., 2010). Therefore, the involvement of both silicified materials in the silicified seafloor and fluid released from basaltic komatiite and komatiite in the basaltic source can explain the decoupled heavy Si but mantle-like O isotope composition of 3.45–3.42 Ga and 3.24–3.23 Ga TTGs.

6. Implication

The tectonic setting for the Barberton TTGs is still controversial (e.g., Grosch & Slama, 2017; Van Kranendonk et al., 2014; Wang, Tang, et al., 2022; Wang, Yang, et al., 2022; Wang et al., 2019, 2020). However, fluid can be released from basaltic komatiite and komatiite in both sagduction and subduction settings (Figure 3) as long as they are transported from deep levels where a temperature of >ca. 700°C can promote dehydration (Hartnady et al., 2022; Tamblyn et al., 2023). The shift from decoupled to coupled Si–O isotopes of Barberton TTGs may indicate the gradual exhaustion of the komatiite-derived fluids. The decoupled Si–O isotope compositions of 3.45–3.42 Ga and 3.24–3.23 Ga TTGs indicate that the hydrous minerals in komatiitic rocks have undergone a dehydration process at that time. In a short time interval (ca. 1 ∼ 10 Myr), the komatiitic rocks are unlikely to erupt underwater and then provide the low-$\delta^{18}O$ fluid again. In contrast, relatively high Dy/Yb ratios (Figure S6 in Supporting Information S1; Wang, Tang, et al., 2022) of the 3.23–3.22 Ga TTGs compared to the 3.45–3.42 Ga and 3.24–3.23 Ga TTGs imply that the komatiitic rocks have been further transported to a deeper level by sagduction or subduction. Therefore, we demonstrate the decoupling of Si–O in zircons of Archean TTGs provides a new perspective for understanding the genesis of continental crust and the evolution of early Earth. Archean granitoids with mantle-like $\delta^{18}O_{zrc}$ values are generally considered to have formed without the involvement of supracrustal

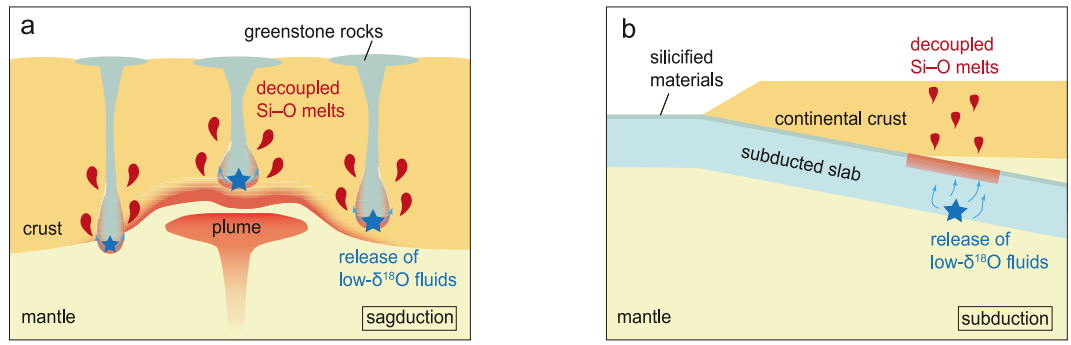

Figure 3. Cartoon models showing the dehydration of basaltic komatiite and komatiite in (a) the sagduction and (b) subduction tectonic settings (modified from Moyen & Martin, 2012).

components (Valley et al., 2005). In addition, the shift from mantle-like to elevated $\delta^{18}O_{zrc}$ values is considered to indicate the initiation of subduction (e.g., Wang, Tang, et al., 2022; Zhang et al., 2018). However, the decoupled Si–O isotopes of the Barberton TTGs show that the mantle-like $\delta^{18}O$ values may have been produced by the addition of both supracrustal silicified materials and fluid from deep basaltic komatiite and komatiite, which indicate that the use only of zircon O isotopes to reveal the genesis of Archean granitoids and the tectonic setting open to various interpretations. The shift of $\delta^{18}O$ values of Archean granitoids may be not related to the tectonic transformation.

7. Conclusions

TTG rocks from the Barberton granitoid-greenstone terrane can be divided into three groups in terms of their formation ages and Si–O isotopes. The 3.45–3.42 Ga (Group 1) and 3.24–3.23 Ga (Group 2) TTGs have mantle-like $\delta^{18}O_{zrc}$ but high $\delta^{30}Si_{melt}$ values, whereas the 3.23–3.22 Ga (Group 3) TTGs are characterized by elevated $\delta^{18}O_{zrc}$ and $\delta^{30}Si_{melt}$ values. We propose that Group 1 and 2 TTGs were formed by the involvement of silicified materials and fluid released from komatiitic rocks and that the formation of Group 3 TTGs involved silicified materials only. We further suggest that the mantle-like O isotope compositions of the Barberton Archean granitoids might not reflect the absence of supracrustal materials.

Data Availability Statement

All analytical data are provided in Tables S1–S5 in Supporting Information S1, which are available on figshare (https://doi.org/10.6084/m9.figshare.23622489.v1).

Acknowledgments
We thank Yu Liu, Guo-Qiang Tang, Xiao-Xiao Ling, Jiao Li, and Sheng He for assistance in acquiring zircon U–Pb and Si–O isotope data, and Hongxia Ma for making sample mounts. We thank Quentin Williams for handling our manuscript as well as two anonymous reviewers for valuable and constructive comments that significantly improved this manuscript. This study was financially supported by the National Natural Science Foundation of China (Grants 41890831, 41973035, and 42025202).

References

Abraham, K., Hofmann, A., Foley, S. F., Cardinal, D., Harris, C., Barth, M. G., & André, L. (2011). Coupled silicon–oxygen isotope fractionation traces Archaean silicification. *Earth and Planetary Science Letters*, *301*(1), 222–230. https://doi.org/10.1016/j.epsl.2010.11.002

André, L., Abraham, K., Hofmann, A., Monin, L., Kleinhanns, I. C., & Foley, S. (2019). Early continental crust generated by reworking of basalts variably silicified by seawater. *Nature Geoscience*, *12*(9), 769–773. https://doi.org/10.1038/s41561-019-0408-5

André, L., Cardinal, D., Alleman, L. Y., & Moorbath, S. (2006). Silicon isotopes in ~3.8 Ga West Greenland rocks as clues to the Eoarchaean supracrustal Si cycle. *Earth and Planetary Science Letters*, *245*(1), 162–173. https://doi.org/10.1016/j.epsl.2006.02.046

André, L., Monin, L., & Hofmann, A. (2022). The origin of early continental crust: New clues from coupling Ge/Si ratios with silicon isotopes. *Earth and Planetary Science Letters*, *582*, 117415. https://doi.org/10.1016/j.epsl.2022.117415

Arndt, N., Lesher, M. C., & Barnes, S. J. (2008). *Komatiite* (p. 487). Cambridge University Press. Retrieved from https://hal-insu.archives-ouvertes.fr/insu-00403305

Boehnke, P., Watson, E. B., Trail, D., Harrison, T. M., & Schmitt, A. K. (2013). Zircon saturation re-revisited. *Chemical Geology*, *351*, 324–334. https://doi.org/10.1016/j.chemgeo.2013.05.028

Byerly, B. L., Kareem, K., Bao, H., & Byerly, G. R. (2017). Early Earth mantle heterogeneity revealed by light oxygen isotopes of Archaean komatiites. *Nature Geoscience*, *10*(11), 871–875. https://doi.org/10.1038/ngeo3054

Chowdhury, W., Trail, D., Miller, M., & Savage, P. (2023). Eoarchean and Hadean melts reveal arc-like trace element and isotopic signatures. *Nature Communications*, *14*(1), 1140. https://doi.org/10.1038/s41467-023-36538-5

Deng, Z., Chaussidon, M., Guitreau, M., Puchtel, I. S., Dauphas, N., & Moynier, F. (2019). An oceanic subduction origin for Archaean granitoids revealed by silicon isotopes. *Nature Geoscience*, *12*(9), 774–778. https://doi.org/10.1038/s41561-019-0407-6

Eiler, J. M. (2001). Oxygen isotope variations of basaltic lavas and upper mantle rocks. *Reviews in Mineralogy and Geochemistry*, *43*(1), 319–364. https://doi.org/10.2138/gsrmg.43.1.319

Frings, P. J., Clymans, W., Fontorbe, G., De La Rocha, C. L., & Conley, D. J. (2016). The continental Si cycle and its impact on the ocean Si isotope budget. *Chemical Geology*, *425*, 12–36. https://doi.org/10.1016/j.chemgeo.2016.01.020

Grosch, E. G., & Slama, J. (2017). Evidence for 3.3-billion-year-old oceanic crust in the Barberton greenstone belt, South Africa. *Geology*, *45*(8), 695–698. https://doi.org/10.1130/g39035.1

Guitreau, M., Gannoun, A., Deng, Z., Chaussidon, M., Moynier, F., Barbarin, B., & Marin-Carbonne, J. (2022). Stable isotope geochemistry of silicon in granitoid zircon. *Geochimica et Cosmochimica Acta*, *316*, 273–294. https://doi.org/10.1016/j.gca.2021.09.029

Guitreau, M., Gannoun, A., Deng, Z., Marin-Carbonne, J., Chaussidon, M., & Moynier, F. (2020). Silicon isotope measurement in zircon by laser ablation multiple collector inductively coupled plasma mass spectrometry. *Journal of Analytical Atomic Spectrometry*, *35*(8), 1597–1606. https://doi.org/10.1039/D0JA00214C

Hammerli, J., Kemp, A. I. S., & Jeon, H. (2018). An Archean Yellowstone? Evidence from extremely low $\delta^{18}O$ in zircons preserved in granulites of the Yilgarn Craton, Western Australia. *Geology*, *46*(5), 411–414. https://doi.org/10.1130/G39969.1

Hartnady, M. I. H., Johnson, T. E., Schorn, S., Hugh Smithies, R., Kirkland, C. L., & Richardson, S. H. (2022). Fluid processes in the early Earth and the growth of continents. *Earth and Planetary Science Letters*, *594*, 117695. https://doi.org/10.1016/j.epsl.2022.117695

Johnson, T. E., Brown, M., Gardiner, N. J., Kirkland, C. L., & Smithies, R. H. (2017). Earth's first stable continents did not form by subduction. *Nature*, *543*(7644), 239–242. https://doi.org/10.1038/nature21383

Johnson, T. E., Kirkland, C. L., Lu, Y., Smithies, R. H., Brown, M., & Hartnady, M. I. H. (2022). Giant impacts and the origin and evolution of continents. *Nature*, *608*(7922), 330–335. https://doi.org/10.1038/s41586-022-04956-y

Kleinhanns, I. C., Kramers, J. D., & Kamber, B. S. (2003). Importance of water for Archaean granitoid petrology: A comparative study of TTG and potassic granitoids from Barberton Mountain Land, South Africa. *Contributions to Mineralogy and Petrology*, *145*(3), 377–389. https://doi.org/10.1007/s00410-003-0459-9

Kröner, A. & Hofmann, A. (Eds.), (2019). (Eds.) *The Archaean geology of the Kaapvaal Craton, southern Africa*. Springer International Publishing. https://doi.org/10.1007/978-3-319-78652-0

Lei, K., Wang, H., Wang, X. L., Zhang, Q., & Li, X.-H. (2023). Supplementary Tables for Lei et al. (2023) submitted to Geophysical Research Letters" by Lei et al [Dataset]. figshare. https://doi.org/10.6084/m9.figshare.23622489.v1

Li, X.-H., Liu, Y., Li, Q.-L., Guo, C.-H., & Chamberlain, K. R. (2009). Precise determination of Phanerozoic zircon Pb/Pb age by multicollector SIMS without external standardization. *Geochemistry, Geophysics, Geosystems*, *10*(4), Q04010. https://doi.org/10.1029/2009GC002400

Li, X.-H., Long, W.-G., Li, Q.-L., Liu, Y., Zheng, Y.-F., Yang, Y.-H., et al. (2010). Penglai zircon megacrysts: A potential new working reference material for microbeam determination of Hf–O isotopes and U–Pb age. *Geostandards and Geoanalytical Research*, *34*(2), 117–134. https://doi.org/10.1111/j.1751-908X.2010.00036.x

Li, X.-H., Tang, G., Gong, B., Yang, Y., Hou, K., Hu, Z., et al. (2013). Qinghu zircon: A working reference for microbeam analysis of U-Pb age and Hf and O isotopes. *Chinese Science Bulletin*, *58*(36), 4647–4654. https://doi.org/10.1007/s11434-013-5932-x

Liou, P., & Guo, J. (2019). Generation of Archaean TTG gneisses through amphibole-dominated fractionation. *Journal of Geophysical Research-Solid Earth*, *124*(4), 3605–3619. https://doi.org/10.1029/2018jb017024

Liu, Y., Li, X.-H., Savage, P. S., Tang, G.-Q., Li, Q.-L., Yu, H.-M., et al. (2022). New quartz and zircon Si isotopic reference materials for precise and accurate SIMS isotopic microanalysis. *Atomic Spectroscopy*, *43*(2), 99–106.

Liu, Y., Li, X.-H., Tang, G.-Q., Li, Q.-L., Liu, X.-C., Yu, H.-M., & Huang, F. (2019). Ultra-high precision silicon isotope micro-analysis using a Cameca IMS-1280 SIMS instrument by eliminating the topography effect. *Journal of Analytical Atomic Spectrometry*, *34*(5), 906–914. https://doi.org/10.1039/c8ja00431e

Lowe, D. R., & Byerly, G. R. (2007). Chapter 5.3 an overview of the geology of the Barberton greenstone belt and vicinity: Implications for early crustal development. In M. J. van Kranendonk, R. H. Smithies, & V. C. Bennett (Eds.), *Developments in precambrian geology* (Vol. 15, pp. 481–526). Elsevier. https://doi.org/10.1016/S0166-2635(07)15053-2

Méheut, M., Lazzeri, M., Balan, E., & Mauri, F. (2007). Equilibrium isotopic fractionation in the kaolinite, quartz, water system: Prediction from first-principles density-functional theory. *Geochimica et Cosmochimica Acta*, *71*(13), 3170–3181. https://doi.org/10.1016/j.gca.2007.04.012

Méheut, M., Lazzeri, M., Balan, E., & Mauri, F. (2009). Structural control over equilibrium silicon and oxygen isotopic fractionation: A first-principles density-functional theory study. *Chemical Geology*, *258*(1), 28–37. https://doi.org/10.1016/j.chemgeo.2008.06.051

Méheut, M., & Schauble, E. A. (2014). Silicon isotope fractionation in silicate minerals: Insights from first-principles models of phyllosilicates, albite and pyrope. *Geochimica et Cosmochimica Acta*, *134*, 137–154. https://doi.org/10.1016/j.gca.2014.02.014

Moyen, J.-F., & Martin, H. (2012). Forty years of TTG research. *Lithos*, *148*, 312–336. https://doi.org/10.1016/j.lithos.2012.06.010

Moyen, J.-F., Stevens, G., Kisters, A. F. M., & Belcher, R. W. (2007). Chapter 5.6 TTG Plutons of the Barberton Granitoid-Greenstone Terrain, South Africa. In M. J. van Kranendonk, R. H. Smithies, & V. C. Bennett (Eds.), *Developments in Precambrian geology* (Vol. 15, pp. 607–667). Elsevier. https://doi.org/10.1016/S0166-2635(07)15056-8

Müntener, O., Kelemen, P. B., & Grove, T. L. (2001). The role of H_2O during crystallization of primitive arc magmas under uppermost mantle conditions and genesis of igneous pyroxenites: An experimental study. *Contributions to Mineralogy and Petrology*, *141*(6), 643–658. https://doi.org/10.1007/s004100100266

Pope, E. C., Bird, D. K., & Arnórsson, S. (2013). Evolution of low-^{18}O Icelandic crust. *Earth and Planetary Science Letters*, *374*, 47–59. https://doi.org/10.1016/j.epsl.2013.04.043

Qin, T., Wu, F., Wu, Z., & Huang, F. (2016). First-principles calculations of equilibrium fractionation of O and Si isotopes in quartz, albite, anorthite, and zircon. *Contributions to Mineralogy and Petrology*, *171*(11), 91. https://doi.org/10.1007/s00410-016-1303-3

Reimink, J. R., Chacko, T., Stern, R. A., & Heaman, L. M. (2014). Earth's earliest evolved crust generated in an Iceland-like setting. *Nature Geoscience*, *7*(7), 529–533. https://doi.org/10.1038/ngeo2170

Robert, F., & Chaussidon, M. (2006). A palaeotemperature curve for the Precambrian oceans based on silicon isotopes in cherts. *Nature*, *443*(7114), 969–972. https://doi.org/10.1038/nature05239

Savage, P. S., Georg, R. B., Armytage, R. M. G., Williams, H. M., & Halliday, A. N. (2010). Silicon isotope homogeneity in the mantle. *Earth and Planetary Science Letters*, *295*(1–2), 139–146. https://doi.org/10.1016/j.epsl.2010.03.035

Savage, P. S., Georg, R. B., Williams, H. M., Burton, K. W., & Halliday, A. N. (2011). Silicon isotope fractionation during magmatic differentiation. *Geochimica et Cosmochimica Acta*, *75*(20), 6124–6139. https://doi.org/10.1016/j.gca.2011.07.043

Savage, P. S., Georg, R. B., Williams, H. M., & Halliday, A. N. (2013). Silicon isotopes in granulite xenoliths: Insights into isotopic fractionation during igneous processes and the composition of the deep continental crust. *Earth and Planetary Science Letters*, *365*, 221–231. https://doi.org/10.1016/j.epsl.2013.01.019

Smithies, R. H., Lu, Y., Kirkland, C. L., Johnson, T. E., Mole, D. R., Champion, D. C., et al. (2021). Oxygen isotopes trace the origins of Earth's earliest continental crust. *Nature*, *592*(7852), 70–75. https://doi.org/10.1038/s41586-021-03337-1

Tamblyn, R., Hermann, J., Hasterok, D., Sossi, P., Pettke, T., & Chatterjee, S. (2023). Hydrated komatiites as a source of water for TTG formation in the Archean. *Earth and Planetary Science Letters*, *603*, 117982. https://doi.org/10.1016/j.epsl.2022.117982

Trail, D., Boehnke, P., Savage, P. S., Liu, M. C., Miller, M. L., & Bindeman, I. (2018). Origin and significance of Si and O isotope heterogeneities in Phanerozoic, Archean, and Hadean zircon. *Proceedings of the National Academy of Sciences of the United States of America*, *115*(41), 10287–10292. https://doi.org/10.1073/pnas.1808335115

Trail, D., Savage, P. S., & Moynier, F. (2019). Experimentally determined Si isotope fractionation between zircon and quartz. *Geochimica et Cosmochimica Acta*, *260*, 257–274. https://doi.org/10.1016/j.gca.2019.06.035

Troch, J., Ellis, B. S., Harris, C., Bachmann, O., & Bindeman, I. N. (2020). Low-δ^{18}O silicic magmas on Earth: A review. *Earth-Science Reviews*, *208*, 103299. https://doi.org/10.1016/j.earscirev.2020.103299

Valley, J. W. (2003). Oxygen isotopes in zircon. *Reviews in Mineralogy and Geochemistry*, *53*(1), 343–385. https://doi.org/10.2113/0530343

Valley, J. W., Lackey, J. S., Cavosie, A. J., Clechenko, C. C., Spicuzza, M. J., Basei, M. A. S., et al. (2005). 4.4 billion years of crustal maturation: Oxygen isotope ratios of magmatic zircon. *Contributions to Mineralogy and Petrology*, *150*(6), 561–580. https://doi.org/10.1007/s00410-005-0025-8

van den Boorn, S. H. J. M., van Bergen, M. J., Nijman, W., & Vroon, P. Z. (2007). Dual role of seawater and hydrothermal fluids in Early Archean chert formation: Evidence from silicon isotopes. *Geology*, *35*(10), 939–942. https://doi.org/10.1130/g24096a.1

van den Boorn, S. H. J. M., van Bergen, M. J., Vroon, P. Z., de Vries, S. T., & Nijman, W. (2010). Silicon isotope and trace element constraints on the origin of ~3.5Ga cherts: Implications for Early Archaean marine environments. *Geochimica et Cosmochimica Acta*, *74*(3), 1077–1103. https://doi.org/10.1016/j.gca.2009.09.009

Van Kranendonk, M. J., Kröner, A., Hoffmann, J. E., Nagel, T., & Anhaeusser, C. R. (2014). Just another drip: Re-Analysis of a proposed mesoarchean suture from the Barberton Mountain Land, South Africa. *Precambrian Research*, *254*, 19–35. https://doi.org/10.1016/j.precamres.2014.07.022

Vermeesch, P. (2018). IsoplotR: A free and open toolbox for geochronology. *Geoscience Frontiers*, *9*(5), 1479–1493. https://doi.org/10.1016/j.gsf.2018.04.001

Vho, A., Lanari, P., Rubatto, D., & Hermann, J. (2020). Tracing fluid transfers in subduction zones: An integrated thermodynamic and δ^{18}O fractionation modelling approach. *Solid Earth*, *11*(2), 307–328. https://doi.org/10.5194/se-11-307-2020

Wang, H., Wilson, A., Yang, J., Li, Q., Tang, G., Feng, L., & Jia, L. (2023). No ^{18}O-depleted mantle source for Archean komatiite. *Science Bulletin*, *68*(1), 53–55. https://doi.org/10.1016/j.scib.2022.12.017

Wang, H., Yang, J.-H., Kröner, A., Zhu, Y.-S., & Li, R. (2019). Non-subduction origin for 3.2 Ga high-pressure metamorphic rocks in the Barberton granitoid-greenstone terrane, South Africa. *Terra Nova*, *31*(4), 373–380. https://doi.org/10.1111/ter.12397

Wang, H., Yang, J.-H., Kröner, A., Zhu, Y.-S., Wei, Q.-D., Li, R., & Xu, L. (2020). Extensive magmatism and metamorphism at ca. 3.2 Ga in the eastern Kaapvaal Craton. *Precambrian Research*, *351*, 105952. https://doi.org/10.1016/j.precamres.2020.105952

Wang, H., Yang, J.-H., Zhu, Y.-S., Huang, C., Xu, L., Wu, S.-T., & Liu, Y. (2022). Archean crustal growth and reworking revealed by combined U-Pb-Hf-O isotope and trace element data of detrital zircons from ancient and modern river sediments of the eastern Kaapvaal Craton. *Geochimica et Cosmochimica Acta*, *320*, 79–104. https://doi.org/10.1016/j.gca.2021.12.025

Wang, X., Tang, M., Moyen, J., Wang, D., Kröner, A., Hawkesworth, C., et al. (2022). The onset of deep recycling of supracrustal materials at the Paleo-Mesoarchean boundary. *National Science Review*, *9*(3), nwab136. https://doi.org/10.1093/nsr/nwab136

Watson, E. B., & Harrison, T. M. (1983). Zircon saturation revisited: Temperature and composition effects in a variety of crustal magma types. *Earth and Planetary Science Letters*, *64*(2), 295–304. https://doi.org/10.1016/0012-821X(83)90211-X

Wiedenbeck, M., Hanchar, J. M., Peck, W. H., Sylvester, P., Valley, J., Whitehouse, M., et al. (2004). Further characterisation of the 91500 zircon crystal. *Geostandards and Geoanalytical Research*, *28*(1), 9–39. https://doi.org/10.1111/j.1751-908X.2004.tb01041.x

Yu, H.-M., Li, Y.-H., Gao, Y.-J., Huang, J., & Huang, F. (2018). Silicon isotopic compositions of altered oceanic crust: Implications for Si isotope heterogeneity in the mantle. *Chemical Geology*, *479*, 1–9. https://doi.org/10.1016/j.chemgeo.2017.12.013

Yu, H.-M., Yang, L., Zhang, G.-L., & Huang, F. (2023). Silicon isotopic compositions of altered Oceanic crust samples from IODP U1365 and U1368: Effect of low-temperature seawater alteration. *Chemical Geology*, *624*, 121424. https://doi.org/10.1016/j.chemgeo.2023.121424

Zhang, J., Zhang, H.-F., Li, L., & Wang, J.-L. (2018). Neoarchean-Paleoproterozoic tectonic evolution of the southern margin of the North China Craton: Insights from geochemical and zircon U–Pb–Hf–O isotopic study of metavolcanic rocks in the Dengfeng complex. *Precambrian Research*, *318*, 103–121. https://doi.org/10.1016/j.precamres.2018.10.008

Zhang, Q., Zhao, L., Zhou, D., Nutman, A. P., Mitchell, R. N., Liu, Y., et al. (2023). No evidence of supracrustal recycling in Si-O isotopes of Earth's oldest rocks 4 Ga ago. *Science Advances*, *9*(26), eadf0693. https://doi.org/10.1126/sciadv.adf0693